

Elena V. Kudryashova · Marcel B. J. Meinders
Antonie J. W. G. Visser · Arie van Hoek
Harmen H. J. de Jongh

Structure and dynamics of egg white ovalbumin adsorbed at the air/water interface

Received: 13 February 2003 / Accepted: 19 March 2003 / Published online: 23 April 2003
© EBSA 2003

Abstract The molecular properties of egg white ovalbumin adsorbed at the air/water interface were studied using infrared reflection absorption spectroscopy (IRRAS) and time-resolved fluorescence anisotropy (TRFA) techniques. Ovalbumin adsorbed at the air/water interface adopts a characteristic partially unfolded conformation in which the content of the β -sheet is 10% lower compared to that of the protein in bulk solution. Adsorption to the interface leads to considerable changes in the rotational dynamics of ovalbumin. The results indicate that the end-over-end mobility of the ellipsoidal protein becomes substantially restricted. This is likely to reflect a preferential orientation of the protein at the interface. Continuous compression of surface layers of ovalbumin causes local aggregation of the protein, resulting in protein–network formation at the interface. The altered protein–protein interactions contribute to the strong increase in surface pressure observed.

Keywords Infrared reflection absorption spectroscopy · Protein structure · Surface compression · Surface layer · Time-resolved fluorescence anisotropy

Introduction

One of the main issues in interface science is to unravel the key mechanisms defining the formation and stability of colloidal systems by the adsorption of surface-active components. In-depth knowledge on the molecular properties of components, like proteins, at air/water or oil/water interfaces is essential in order to elucidate the mechanisms behind the formation and stability of foams and emulsions, and to understand the protein specificity in these mechanisms. It has been reported that proteins spontaneously adsorb from an aqueous solution to the air/water interface, probably due to energetically favorable dehydration of hydrophobic regions of the protein surface. It is generally believed that, upon adsorption, globular proteins unfold and form an interfacial surface layer exhibiting viscoelastic properties (Graham and Philips 1979, 1980; Pezennec et al. 2000). To study the molecular characteristics of proteins adsorbed at the interfaces, various techniques have been used during the last decade, including ellipsometry, neutron and X-ray reflectivity, circular dichroism, fluorescence microscopy, atomic force and near-field optical microscopies (Dickinson et al. 1993; Kopelman and Tan 1993; Atkinson et al. 1995; Gunning et al. 1996; Visser 1997; Elwing 1998; Harzallah et al. 1998; de Jongh and Meinders 2002). In a few studies, Blodgett films were used to study the conformation and aggregation state of proteins at interfaces (e.g. Wustneck et al. 1996; Blaudez et al. 1999; Pezennec et al. 2000), but on-line measurements have not been published thus far.

It has been recently demonstrated (Meinders et al. 2000, 2001; Meinders and de Jongh 2002) that infrared reflection absorption spectroscopy (IRRAS) can provide detailed information on the molecular properties of

M. B. J. Meinders · H. H. J. de Jongh (✉)
Wageningen Centre for Food Sciences, Diedenweg 20,
6703 GW Wageningen, The Netherlands
E-mail: harmen.dejongh@wur.nl
Tel.: +31-317-482101
Fax: +31-317-484893

E. V. Kudryashova
Division of Chemical Enzymology, Chemistry Department,
Moscow State University, 119899 Moscow, Russia

M. B. J. Meinders
Agrotechnological Research Institute, Bornsesteeg 59,
Wageningen, The Netherlands

A. J. W. G. Visser · A. van Hoek
Microspectroscopy Centre,
Laboratories of Biochemistry and Biophysics,
Wageningen University, Dreijenlaan 3,
6703 HA Wageningen, The Netherlands

H. H. J. de Jongh
TNO Nutrition and Food Research Institute,
Utrechtseweg 48, Zeist, The Netherlands

proteins adsorbed at the air/water interface, such as the concentration of the protein at and near the interface, the thickness of the surface layer and the protein secondary structure in this layer. This technique has an estimated penetration depth of 400–500 nm and allows the analysis of relatively thick surface layers. Time-resolved fluorescence anisotropy (TRFA) measurements allow the monitoring of the internal and overall rotational dynamics of proteins and yields information on the protein spatial structure, like domain structure or protein aggregation state. While TRFA is widely used to study protein structure in solution (Szabo 1984; Brand et al. 1985; Vos et al. 1987; Digris et al. 1999; Lakowicz 1999; Kudryashova et al. 2001, 2002), this paper is the first report on the application of fluorescence in external reflection mode to study the properties of proteins adsorbed at the air/water interface.

In this work we focus attention on the structural properties of egg white ovalbumin, a protein often applied in food colloidal systems. Both the conformational and dynamic properties of this protein adsorbed to air/water interfaces are studied using two spectroscopic methods (IRRAS and TRFA) in combination with Langmuir balance measurements. We demonstrate that the combination of both approaches provides new insights into protein structural changes upon adsorption at the air/water interface and under conditions of surface layer compression at a protein molecular level in relation to surface rheological data. Such insights might contribute to the understanding of the protein specificity observed in foam formation and stabilization.

Materials and methods

Ovalbumin purification

Ovalbumin was purified from fresh hen eggs using the following semi-large-scale procedure. The egg white and yolk from nine eggs were separated by hand. To the egg white fraction, which had a volume of 300 mL, 600 mL of a 50 mM Tris-HCl buffer (pH 7.5) containing 5 mM β -mercaptoethanol was added. This solution was stirred for 24 h at 4 °C. Subsequently, the solution was centrifuged for 30 min at 14,000 rpm and 4 °C. The pellet was discarded, while 1800 mL of 50 mM Tris-HCl (pH 7.5) was added to the supernatant. After a period of 30 min gentle stirring, the solution was filtered over a paper filter and subsequently 500 g of DEAE Sephadex Cl-6B (Pharmacia) was added, followed by overnight incubation at 4 °C under gentle stirring. Next, the solution was filtered over a glass filter (G2) followed by extensive washing with 10 L demineralized water and, subsequently, 5 L 0.1 M NaCl. Next, the protein was eluted stepwise with respectively 1 L of 0.1, 0.15, 0.2, 0.25 and 0.35 M NaCl. The 0.15, 0.2 and 0.25 M NaCl fractions were pooled and concentrated using a Diaflow Ultrafiltration Device with a 10 kDa molecular weight cut-off membrane. The concentrated solution was dialyzed extensively against demineralized water and freeze-dried. The freeze-dried ovalbumin (yield 8 g) was stored at –20 °C.

SDS-PAGE was performed on homogeneous 15% slabgels using a Mini-PROTEAN II Electrophoresis system (BioRad). Samples were dissolved in sample buffer containing 62.5 mM Tris-HCl (pH 6.8), 1.25% SDS, 5% glycerol, 0.00125% bromophenol blue and 1.25% β -mercaptoethanol and heated for 10 min at 100 °C prior to analysis. The slabgels were fixed and stained in

0.1% Coomassie Brilliant Blue R-250 in 40% methanol/10% acetic acid solution and de-stained in 30% methanol/10% acetic acid solution. The protein had a purity higher than 98%, based on densitometric analysis of the gel.

Langmuir trough experiments

An automated computer-interfaced Teflon Langmuir trough (NIMA 601M, UK) was used, with two compartments for the sample and reference solutions, respectively. The sample compartment was equipped with two moving barriers. The dimensions of the Langmuir trough were 10×26 cm (390 mL) for the sample compartment and 5×26 cm (195 mL) for the reference compartment. A pressure sensor (Langmuir balance) connected to a paper Wilhelmy plate measured the surface pressure. Prior to a measurement, the balance was calibrated using standard weights. The surface tension (σ_0) of the buffer solution in the reference compartment was 72.2 mN/m.

Typically, 390 mL of a protein solution ranging from 0.1 to 50 mg/mL in 10 mM phosphate buffer (pH 7.0; using Millipore water) was transferred to the sample compartment. After cleaning the surface using a sucking device with a micro-tip, the surface pressure ($\pi = \sigma - \sigma_0$) of the protein solution was followed as a function of time. The pressure-area (π - A) isotherms were recorded at a barrier speed of 3–6 cm/min, depending on the maximal area used, to obtain compression rates of about 20% of the initial area per minute (in our studies the maximal area is 230 cm²). Simultaneously, IRRAS or TRFA measurements were performed. All experiments were carried out at 22 ± 0.5 °C.

IRRAS measurements

Spectra acquisition

IRRAS spectra were acquired using an Equinox 50 FTIR spectrometer attached to an external reflection module (Bruker XA-500) and equipped with a liquid nitrogen cooled MCT detector. The spectrometer was placed on an optical bench table to minimize and dampen external vibrations. The incident and refracting angle of the infrared beam was 30° in all experiments described here. The FTIR spectrometer was purged with a constant flow of dry air. For the recording of attenuated total reflection (ATR) spectra a BioRad FTS 6000 spectrometer was used equipped with an MCT detector using a germanium crystal (45°, trapezoid, six internal total reflections). The experimental equipment and measurement procedure have been described in detail elsewhere (Meinders et al. 2000, 2001). Fourier transform infrared (FTIR) spectra (ATR and IRRAS) were acquired from 1000 to 4000 cm⁻¹ with 2 cm⁻¹ spectral resolution. For each spectrum, 100 scans were accumulated at 20 kHz scanning speed and averaged. Reference spectra of protein-free samples were recorded under identical conditions. External reflection absorption spectra of the protein are presented as $-\log(R_{\text{prot}}/R_{\text{buf}})$, where R_{prot} is the reflection spectrum of the protein solution and R_{buf} is the reflection spectrum of the buffer solution. The resultant spectra were smoothed with a nine-point Savitsky-Golay smooth function to approximately 8 cm⁻¹.

Spectral simulation

To extract the information on the molecular properties of the protein at the interface from IRRAS spectra, the experimental spectra were simulated using absorption spectra as input. The spectral simulation was carried out using recently developed software described by Meinders et al. (2001) and based on the optical theory widely used for the analysis of the data in ellipsometry, X-ray and neutron reflectometry to determine layer thickness, density profiles and optical parameters (Yamamoto and Ishida 1994). The details of the theory and application of the procedure

for simulation of IRRAS spectra are described elsewhere (Meinders et al. 2000, 2001).

In short, the spectral simulation method is based on the stratified layer model, considering a system consisting of a several homogeneous layers (N) with a particular thickness (d) over the solution. The optical properties of each layer are described by the complex refractive index (\hat{n}). For layer j this is defined as $\hat{n}_j = n_j + ik_j$ and is a function of the wavelength (ν). The real part n_j is the refractive index. The imaginary part k_j is the extinction coefficient that is related to the absorption coefficient α by $\alpha = 4\pi k/\lambda$, with λ being the wavelength of the light. It is the absorption coefficient that is measured in ATR experiments. The ATR spectrum of a protein is used to represent the imaginary part of the complex refractive index (the extinction coefficient k_j of the protein). The real part of the refractive index can be calculated from the imaginary part using the Kramers–Kronig relation:

$$n(\nu) = n(\infty) + \frac{2}{\pi} \int_0^{\infty} \frac{\nu' k(\nu')}{\nu'^2 - \nu^2} d\nu' \quad (1)$$

where $n(\infty)$ is the baseline refractive index. Using the Kramers–Kronig transformation, the complex refractive index of the protein solution can be related to the reflection spectrum, $R(\nu)$. This analysis is widely used and has been published elsewhere (Bardwell and Dignam 1985), while here we only show the relevant equations:

$$\phi(\nu) = \frac{2\nu}{\pi} \int_0^{\infty} \frac{\ln \sqrt{R(\nu')}}{\nu'^2 - \nu^2} d\nu' \quad (2)$$

where ϕ is the phase shift.

$$\hat{r} = \sqrt{R} e^{i\phi} \quad (3)$$

where \hat{r} is the complex reflection coefficient and R is the reflectivity.

$$\hat{n}_1 = \hat{n}_0 \sqrt{\sin^2 \theta_0 + \left(\frac{\hat{r} - 1}{\hat{r} + 1} \right)^2 \cos^2 \theta_0} \quad (4)$$

where \hat{n}_0 and \hat{n}_1 are the refracting indices of the incidence and reflecting medium, respectively, while θ_0 and θ_1 are the angles of incidence and refraction, respectively (given for optical configuration with only one reflecting surface and for s-polarization). In our case the incidence medium is air, giving $\hat{n}_0 = n_0 = 1$ and $\theta_0 = \theta_1$ becomes real.

Based on this theory, the simulation IRRAS spectra can be composed using absorption spectra (ATR-FTIR) as input. The fit parameters are the proportionality constant relating the protein ATR/absorption spectrum and the protein extinction coefficient, the number of layers N , the concentration of the protein c_j for each layer, and thickness d_j of the layers above the substrate ($1 \leq j < N$). In our case the system can be satisfactorily described by air, a top surface layer and a sub-phase. The introduction of additional layers did not provide a better description of the IRRAS spectra, while using a system consisting of only a single layer was not sufficient to describe the spectra adequately. Hence, spectral simulation in our case yields the top layer thickness (d), surface (or interface) and sub-phase protein concentrations (respectively c_1 and c_2). The uncertainty in the fitting parameters is generally in the order of 10–30%, depending on the bulk concentration (for higher concentrations a broader concentration range describes the IRRAS spectra equally well).

The secondary structure of the protein in the surface layer was analyzed using spectral simulation by adjusting the ATR spectrum, with reference spectra representing the secondary structure contributions (for example –10% β -strand and +10% random coil). The new composed absorption spectrum was then used as input spectrum in the analysis. The details of the application of the simulation procedure have been described before (Meinders et al. 2000, 2001). In a similar way, the degree of aggregation of the protein adsorbed at the interface was estimated, taking into

account the anti-parallel β -sheet structure as an additional component of the secondary structure of the protein. It has been shown (Dong et al. 2000) that aggregation of ovalbumin is accompanied with the formation of anti-parallel β -sheets, which is characterized by the peak wavelengths in the amide I region (1624 and 1693 cm^{-1}) well distinct from the parallel β -structures (1638 and 1686 cm^{-1}). The formation of the anti-parallel β -structure was used as a criterion for evaluation of the degree of aggregation of ovalbumin at the interface.

TRFA measurements

TRFA measurements were carried out using mode-locked continuous wave lasers for excitation and time-correlated single photon counting as the detection technique. The measurements in cuvettes were carried out as described before (Kudryashova et al. 2001). The frequency of excitation pulses was 951.2 kHz; the excitation wavelength was 300 nm. For fluorescence and anisotropy lifetime measurements of the protein adsorbed at the air/water interface (in the Langmuir trough), the setup was slightly adapted (see Fig. 1). The polarization direction of the excitation beam was changed to the horizontal, parallel to the plane of the interface; the beam was grazing the interface at 80° with respect to the normal. The detection direction was vertical. A set of two identical lenses was used to collect the fluorescence of the boundary layer and then focus that fluorescence at the input slit of a double monochromator (CVI, Albuquerque, NM, USA, model CM 112, with the gratings in a subtractive dispersion configuration). Between these lenses a computer-controlled sheet-type polarizer was placed to select the parallel and perpendicularly polarized components of fluorescence. The light output of the monochromator was focused on the cathode of a Hamamatsu model R3809U-50 photomultiplier and the rest of the detection chain was similar to that described by Kudryashova et al. (2001). For deconvolution purposes in the case of measurements at the Langmuir-trough surface layer, the scattered excitation light at the surface layer was used. The temperature of all experiments was $22 \pm 0.5^\circ \text{C}$.

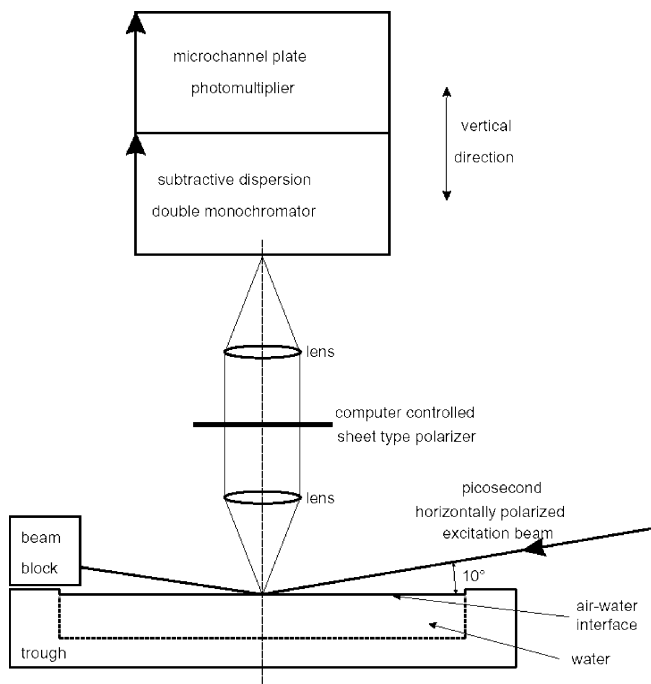


Fig. 1 Schematic view of TRFA setup in reflection mode combined with a Langmuir trough to measure the dynamic fluorescence properties of proteins at the air/water interface. The surface pressure was measured on-line using a Wilhelmy balance

Data analysis was performed using a home-built computer program (Digris et al. 1999; Novikov et al. 1999). For the experiments in cuvettes, the analysis of the data was carried out as described before (Kudryashova et al. 2001). For the experiments in the Langmuir trough, a 2D-anisotropy model was used for the anisotropy decay analysis. Since in a 2D system the anisotropy and degree of polarization are equal (Morrison and Weber 1987), the anisotropy decay is described as:

$$r(t) = \frac{I_{\parallel}(t) - gI_{\perp}(t)}{I_{\parallel}(t) + gI_{\perp}(t)} \quad (5)$$

where I_{\parallel} and I_{\perp} are the polarized emission intensities parallel and perpendicular to the polarized excitation direction; g is the factor accounting for the sensitivity of the detection system for the perpendicular component with respect to the parallel one. The g -factor has been determined in a tail-matching procedure of the parallel and perpendicularly polarized fluorescence decays of a small, fast rotating dye molecule (*para*-terphenyl) in cyclohexane. Data analysis in discrete exponential terms was performed using the TRFA Data Processing Package of the Scientific Software Technologies Center (Belarusian State University, Belarus). First the fluorescence lifetime profile consisting of a sum of discrete exponentials with lifetime τ_i and amplitude α_i can be retrieved from the total fluorescence according to the relation:

$$I(t) = I_{\parallel}(t) + g * I_{\perp}(t) = E(t) * \sum_{i=1}^N \alpha_i e^{-t/\tau_i} \quad (6)$$

where $E(t)$ is the instrumental response function and N is the number of fluorescent components.

In global analysis of the fluorescence anisotropy, the time-dependent fluorescence anisotropy $r(t)$ is calculated from the parallel $I_{\parallel}(t)$ and perpendicular $I_{\perp}(t)$ components through the relations (Lakowicz 1999):

$$\begin{aligned} I_{\parallel}(t) &= 1/3 \sum_{i=1}^N \alpha_i e^{-t/\tau_i} \left(1 + g \sum_{j=1}^M r_{0j} e^{-t/\phi_j} \right) \text{ and } I_{\perp}(t) \\ &= 1/3 \sum_{i=1}^N \alpha_i e^{-t/\tau_i} \left(1 - g \sum_{j=1}^M r_{0j} e^{-t/\phi_j} \right) \end{aligned} \quad (7)$$

in which we assume that all fluorescence lifetimes equally contribute to the anisotropy. N and M are the number of fluorescent and anisotropy components, respectively. The time dependence of the anisotropy [$r(t)$] (after δ -pulse excitation) can be described by a sum of discrete exponentials with rotational correlation time ϕ_j and initial anisotropy r_{0j} :

$$r(t) = \sum_{j=1}^M r_{0j} e^{-t/\phi_j} \quad (8)$$

The analysis of the data was performed in an iterative fashion until the chi-square was minimized and the weighted residuals between experimental and fitted data and the autocorrelation function between the residuals were randomly distributed around zero. The error of the fitting parameters was determined at the 67% confidence level.

Results

FTIR-ATR spectroscopy

Figure 2A shows the ATR absorption spectrum of an ovalbumin film spread from a protein solution (pH 7.0) on a germanium reflection element and subsequently dried to the air. The protein amide A bands can be

observed around 3000–3300 cm^{-1} and the amide I and II bands are present between 1600–1700 and 1500–1600 cm^{-1} , respectively (see lower graph for enlargement). The band shape of the amide I is known to be sensitive to the protein secondary structure content, and the wavelengths corresponding to the maximal intensity of the individual secondary structure contributions in ovalbumin are indicated in the figure as well (insert). Self-deconvolution of the amide I region to estimate the secondary structure content of ovalbumin was performed using GRAMS/IR software (Buck Scientific) using peak assignments as described elsewhere (Goormaghtigh et al. 1994; Dong et al. 2000). According to such analysis, ovalbumin contains about 47% of β -strands and 35% of α -helix, which is in close agreement with literature data (Stein et al. 1991). Comparison of the amide I band shape of this ATR spectrum with that of a highly concentrated aqueous solution on top of the ATR crystal (results not shown) demonstrated that drying of the protein film for the ATR measurement had no significant effect on the secondary structure content of the protein. Since the ATR spectrum of the protein film is essentially “free” of water contributions, this spectrum is used as the input spectrum in the spectral simulation of IRRAS spectra of ovalbumin as described below.

Infrared reflection absorption spectroscopy

The IRRAS spectrum of ovalbumin at a bulk concentration of 10 mg/mL is shown in Fig. 2B, with the enlargement of the amide I and II regions in the lower panel. In contrast to the ATR spectrum, the protein bands in the IRRAS spectrum are pointed downwards. Around 3500 cm^{-1} , a water contribution can be identified with an opposite sign compared to the protein bands. This is due to the fact that the spectrum of the protein sample is measured relative to that of the protein-free sample and the opposite signs illustrate the depletion of water from the interface by the volume occupied by protein. The water intensity around 3500 cm^{-1} implies that also in the amide I region a water contribution must be apparent, explaining why the amide I and II bands show a comparable intensity, in contrast to, for example, the ATR spectrum (Fig. 2A). IRRAS spectra measured for various bulk concentrations of ovalbumin are shown in Fig. 3. These spectra were measured after an incubation time of 60 min, corresponding to the conditions of quasi-equilibrium where the surface pressure did not change in time (not shown). It can be observed that both the intensity of the amide I and II protein bands and the water intensity increased with increasing bulk protein concentration. Besides, while at low protein concentration the amide I and amide II bands appear more like “absorption” bands, at high protein concentration a positive derivative-like band shape around 1700 cm^{-1} and a negative derivative-like band at 3700 cm^{-1} are observed. These

Fig. 2 **A** FTIR-ATR spectrum of ovalbumin film dried from 100 μL of a 10 mg/mL solution of ovalbumin in 10 mM phosphate buffer (pH 7.0). **B** The IRRAS spectrum of ovalbumin at a bulk concentration of 10 mg/mL in 10 mM phosphate buffer (pH 7.0) after an equilibration time of 60 min. The lower panels show enlargements of the amide I and II regions. The inset in the lower panel of **A** displays the amide I region from 1700 to 1600 cm^{-1} and the contributions of the different secondary structure types (α =alpha helix, β =beta sheet, R =random coil) are indicated

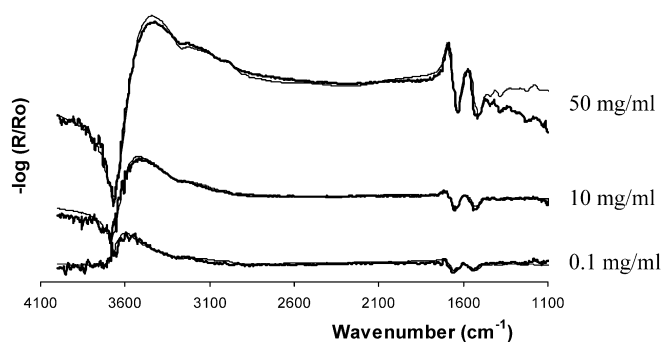
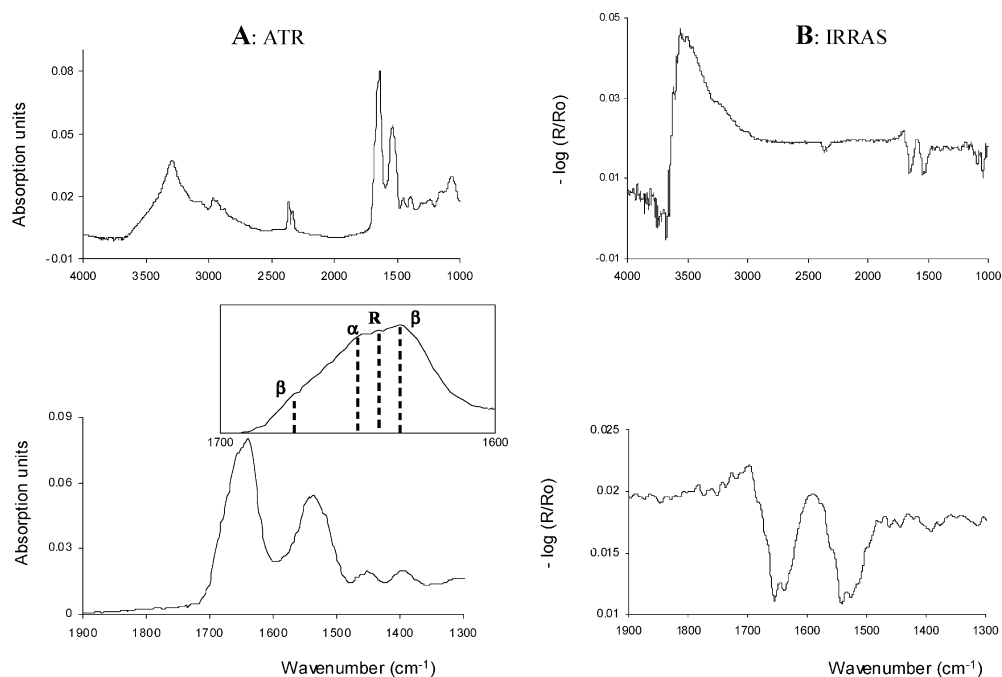


Fig. 3 IRRAS spectra of ovalbumin measured for bulk protein concentrations of 0.1, 10 and 50 mg/mL after adsorption during 60 min. The thin lines represent the simulated spectra as described in the text. The spectra are displaced vertically for clarity reasons

latter features are characteristic for reflection spectra and their intensities correlate to the difference in the protein concentration between the surface layer and the sub-phase (Meinders et al. 2001). For a correct evaluation of the absolute intensity of the protein features and the band shape of the amide I region of the IRRAS spectra, spectral simulation is required of both the water and protein contributions.

The IRRAS spectral simulation is based on a stratified layer model, considering a system consisting of top surface layer in contact with air, and a sub-phase. A detailed description of the simulation method has been published elsewhere (Meinders et al. 2001). Introduction of additional layers in the model did not provide a significantly better description of the IRRAS spectra and are therefore omitted. The simulated IRRAS spectra for different ovalbumin bulk concentrations are also shown in Fig. 3 (thin lines) and the corresponding parameters

Table 1 The simulation parameters obtained from global analysis of IRRAS spectra for different protein bulk concentrations of ovalbumin: protein concentration in the surface layer (C_1), protein concentration in the sub-phase (C_2), surface layer thickness (d)

	0.1 mg/mL	10 mg/mL	50 mg/mL
C_1 (mg/ml)	17	111	236
C_2 (mg/ml)	~ 0.1	16	86
d (nm)	350	90	85

are presented in Table 1. Adsorption of ovalbumin at the air/water interface leads to the formation of a protein-rich surface layer (80–400 nm, depending on the bulk protein concentration and the incubation time; the latter dependence is not shown here) and a sub-phase in which the protein concentration is equal or slightly higher than the original bulk concentration. This latter could be a reflection of an actual concentration gradient of the surface layer, rather than the discrete stratified layers used to describe the system in the spectral simulation. With increasing bulk concentration the surface layer concentration increases, while the ratio of the protein concentration in the surface layer and sub-phase decreases.

In Fig. 4 the amide I regions of the experimental and simulated IRRAS spectra are shown in more detail for different bulk protein concentrations. It can be observed that for bulk protein concentrations of 0.1 and 10 mg/mL the simulated IRRAS spectra (Fig. 4A and B, curves “Sim”) using the native ovalbumin structure as input (ATR spectrum) are characterized by a larger intensity around 1635 cm^{-1} with a shoulder around 1655 cm^{-1} , which is opposite to what is observed in the experimental spectrum (curves “Exp”). Correction of the input

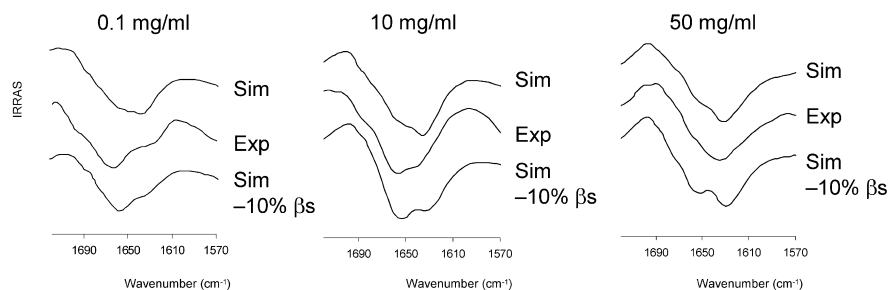


Fig. 4 Evaluation of the secondary structure in ovalbumin adsorbed at the air/water interface by band shape analysis of the amide I region of IRRAS spectra recorded after 60 min for 0.1, 10 and 50 mg/mL bulk concentrations. Curves “Exp” correspond to experimental IRRAS spectra; curves “Sim” correspond to simulated IRRAS spectra without conformational changes; curves “Sim–10% β s” corresponds to simulated IRRAS spectra in which 10% of the β -sheets is transformed into random coil

spectrum by subtracting a theoretical 10% parallel β -strand contribution and adding a theoretical 10% random coil contribution, and using this adapted “absorption” spectrum as input for the IRRAS spectral simulation (see Meinders et al. 2001), gives the curves at the bottom of Fig. 4. These latter simulations describe clearly the experimental spectrum much better in the amide I region for these systems. A 5% or 15% secondary structure correction provides significantly worse comparisons with the experimental spectra (not shown). From this we conclude that, for bulk concentrations ranging from 0.1 to 10 mg/mL, ovalbumin adsorbed at the interface undergoes a small but significant conformational change at a secondary folding level. Only at high protein bulk concentration (50 mg/mL; Fig. 4C) are no indications found that ovalbumin loses the native conformation at the interface, since the simulated IRRAS spectrum without any conformational change taken into account corresponds closer to the experimental IRRAS spectrum than the simulated spectrum including a decrease in β -sheet content.

Time-resolved fluorescence anisotropy

To obtain more insight into the dynamic protein characteristics at the air/water interface, the rotational dynamics were studied using TRFA. Analysis of fluorescence anisotropy decay provides information on internal and overall rotational mobility of the protein: the relatively fast rotation of protein segments, the slower rotation of the whole protein molecule or the very slow rotation of protein complexes (Brand et al. 1985; Lakowicz 1999; Kudryashova et al. 2001). The molecular volume of each rotational fragment can be estimated using the Stokes–Einstein relation. Examples of experimental and fitted total fluorescence and fluorescence anisotropy decays are shown in Fig. 5 for ovalbumin in bulk solution (A) and adsorbed at the air/water interface (B). Table 2 summarizes the parameters (fluorescence lifetimes and rotational correlation times) obtained from

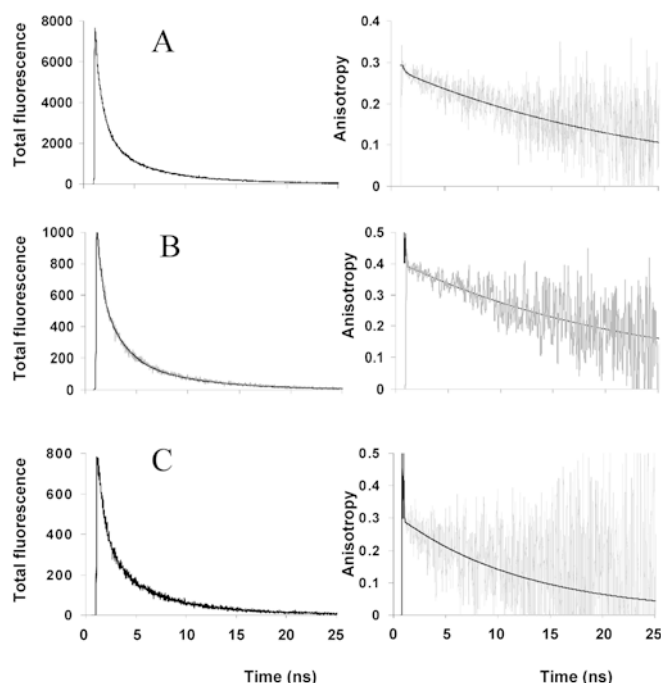


Fig. 5 Total fluorescence and fluorescence anisotropy decays for ovalbumin in the bulk solution (A); for ovalbumin adsorbed at the air/water interface in non-compressed film (B); and under compression of the film from 230 to 155 cm² (C). Bulk protein concentration is 0.1 mg/mL. In all panels the fitted and experimental curves (total fluorescence *left*, anisotropy *right*) are shown

Table 2 Estimated fluorescence and anisotropy decay parameters: fluorescence lifetimes (τ_i) and their relative contributions (α_i), rotational correlation times (ϕ_i) and their relative contributions (β_i) of ovalbumin in the bulk, when adsorbed to an air/water interface in equilibrium or upon compression of the surface layer by reducing the available area by a factor 1.5. The excitation wavelength is 300 nm and the emission wavelength is 343 nm

	β_1	ϕ_1 (ns)	α_1	τ_1 (ns)	α_2	τ_2 (ns)	α_3	τ_3 (ns)
Bulk	0.30	24 ± 1	0.7	0.3	0.15	2.5	0.1	7.2
Interface at equilibrium	0.35	18 ± 2	0.45	0.35	0.4	2.0	0.15	6.9
Interface upon compression	0.30	8.5 ± 2.5	0.6	0.4	0.25	2.0	0.1	7.0

global analysis of the total fluorescence and fluorescence anisotropy decay. It was found that adsorption at the air/water interface hardly affected the fluorescence lifetimes of the protein, while the rotational correlation time is changed significantly (Table 2). This implies

significant changes in the rotational dynamics of ovalbumin upon adsorption. In bulk solution, ovalbumin rotates as a compact monomer. Its rotational correlation time (24 ns) is in good agreement with that expected for a protein with a molecular weight of 43 kDa, like ovalbumin. Interestingly, the protein adsorbed at the interface shows an approximate 1.5 times shorter rotational correlation time (~ 18 ns) compared to that of the protein in bulk solution. This rotational correlation time of ovalbumin adsorbed at the interface remained unchanged during at least the first 2 h of equilibration (results not shown).

Surface layer compression

The combination of IRRAS and TRFA was also applied to study the structure and rotational dynamics of ovalbumin upon continuous compression of a surface layer formed after 1 h of equilibration. The pressure–area isotherm obtained by compression of the available area is presented in Fig. 6. It can be observed that initial compression of the surface layer from 220 to about 150 cm^2 results in a steady increase of the surface pressure. When the available area is further reduced, the surface pressure increases sharply. Further compression to and below 100 cm^2 causes the surface layer to collapse, as illustrated by the leveling-off of the surface pressure.

Analysis of IRRAS spectra recorded at various stages during the compression shows that upon compression of the surface layer from a surface area of 230 to 170 cm^2 the surface concentration as well as the layer thickness is not changed (Fig. 7A). Upon further compression the protein surface concentration starts to increase, while the layer thickness decreases. Band shape analysis of the amide I in the IRRAS spectra shows that no further unfolding of the protein is observed upon compression (with respect to the characteristic partially unfolded

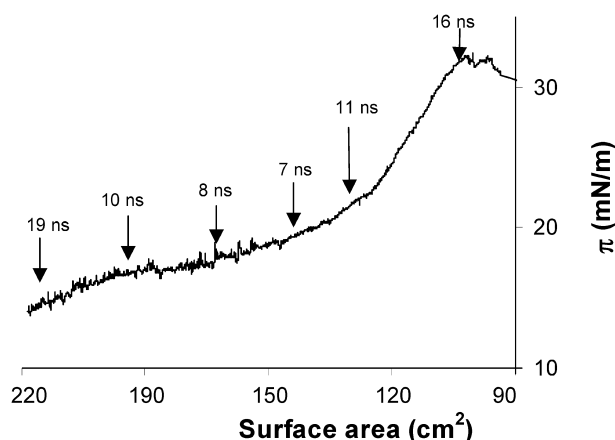


Fig. 6 Pressure–area isotherm obtained by the compression of the film after adsorption during 60 min of ovalbumin from a bulk concentration of 0.1 mg/mL. The rotational correlation times (ϕ , ns) of ovalbumin determined by TRFA as a function of the protein molecular area changing upon the film compression are indicated

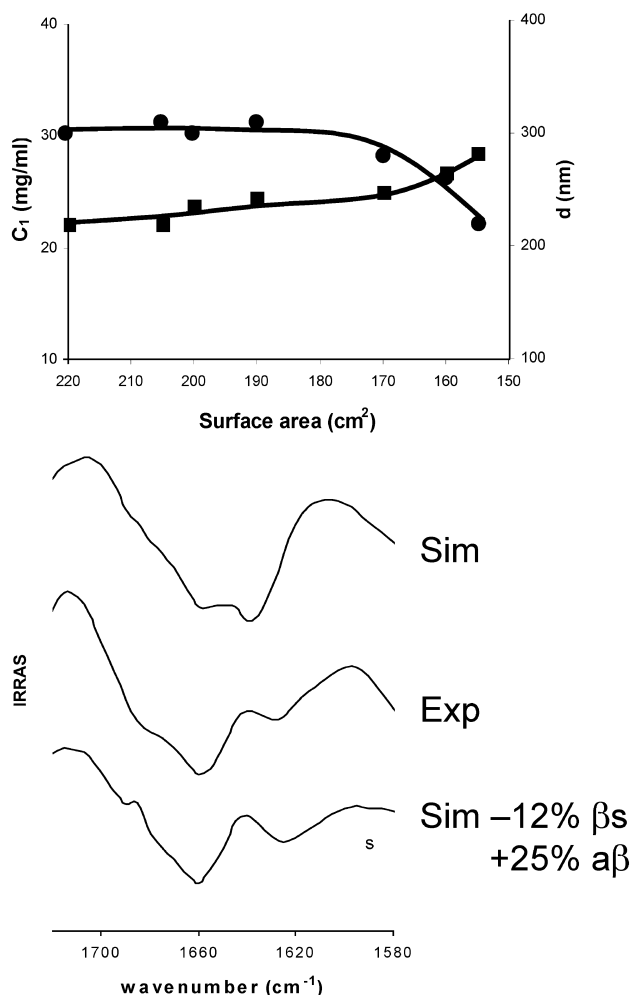


Fig. 7 A Protein concentration in the surface layer (*squares*) and surface layer thickness (*circles*) evaluated from IRRAS as a function of the surface area upon compression of the film. B Evaluation of secondary structure and degree of aggregation from the amide I region of IRRAS spectra of ovalbumin at the air/water interface after compression of the film area from 230 to 155 cm^2 . Curve “exp” corresponds to experimental IRRAS spectrum; curve “sim” corresponds to simulated IRRAS spectra without conformational changes; curve “sim–12% β s +25% $\alpha\beta$ ” corresponds to simulated IRRAS spectra in which the conformational changes are taken into account. Ovalbumin bulk concentration is 0.1 mg/mL

conformation of adsorbed ovalbumin): the content of the parallel β -sheets in ovalbumin is practically the same (the difference between a conversion of 10% or 12% is not regarded significant) (Fig. 7B). In the experimental spectrum of the compressed surface layer (curve “Exp”), however, a distinct shoulder at 1624 cm^{-1} , not present in the “normal” simulated spectra, can be observed. Such a feature is characteristic for the presence of anti-parallel β -sheet formation and its appearance in IR spectra suggests extensive protein aggregation (Dong et al. 2000).

In the ATR spectrum of ovalbumin subjected to heat treatment (1 mg/mL, 15 min at 90 $^{\circ}\text{C}$ at pH 7.0), shown by gel electrophoretic analysis to be effective in

converting all the protein present to an aggregated form (not shown), this anti-parallel β -sheet contribution is also clearly apparent (not shown). Band shape analysis, performed as described above, demonstrated that this fully aggregated material contains about 30% anti-parallel β -sheet. The degree of aggregation of ovalbumin at the interface can then be defined as the ratio between the anti-parallel β -sheet contribution estimated from analysis of the amide I region of the IRRAS spectra relative to this 30% present in the aggregated material subjected to heat treatment. The anti-parallel β -sheet percentage was obtained from IRRAS spectra by spectral simulation, where additionally a contribution of anti-parallel β -sheets to the secondary structure of the protein was taken into account as described in the Materials and methods section. Figure 8 shows the change in the degree of aggregation of ovalbumin upon compression of the film. The degree of aggregation rises from 0 to 85% upon a 1.5-fold reduction of the available surface area. Unfortunately, in the current set-up it was not possible to compress the film to an area less than 150 cm², since the available surface area becomes too small to allow a proper recording of an IRRAS spectrum together with an on-line registration of the surface pressure.

TRFA experiments show that the rotational dynamics of ovalbumin changed strongly upon compression of the film. The values are indicated in Fig. 6 at various stages during the compression. An example of the total fluorescence and fluorescence anisotropy decays of ovalbumin obtained upon compression of the surface layer to an area of 155 cm² is shown in Fig. 5C. It can be observed that compression of the surface layer by reducing the available area from 230 to 150 cm² results in a shorter rotational correlation time compared to the non-compressed film (Table 2, Fig. 6). Upon further compression, these values increase again.

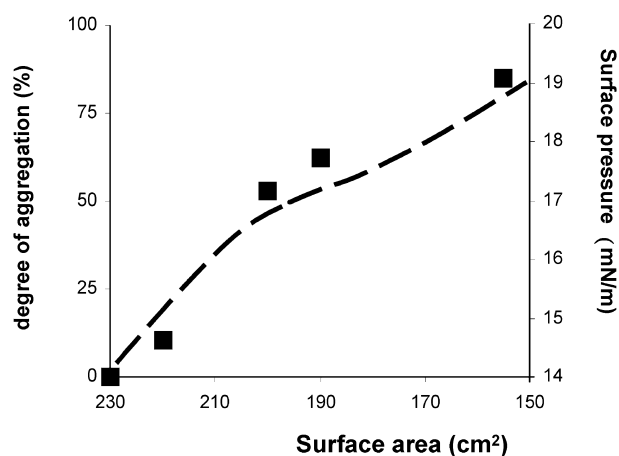


Fig. 8 Correlation between the degree of aggregation of ovalbumin at the air/water interface as deduced from IRRAS spectra, determined by the fraction of anti-parallel β -sheet (sharp intensity at 1624 cm⁻¹ in IRRAS spectra) relative to that present in thermo-aggregated ovalbumin (*squares*) and the surface pressure as determined simultaneously using a Wilhelmy balance (*dashed line*). The ovalbumin bulk concentration is 0.1 mg/mL

Discussion

In this work we aimed to study the molecular properties of ovalbumin at the air/water interface both under equilibrium conditions and upon surface compression using a combination of external reflection infrared and fluorescence techniques. Combining these experiments with on-line detection of the surface pressure provides relations between molecular and rheological properties of the system.

Surface layers in equilibrium

IRRAS measurements have been performed on surface layers after 1 h of equilibration. It was shown that ovalbumin adsorbed at the interface adopts a characteristic partially unfolded conformation in which the β -sheet content is reduced by 10% compared to the native protein in the bulk solution (Fig. 4). This partially unfolded conformation is unchanged over adsorption from a wide range of bulk concentrations (from 0.1 to 10 mg/mL). The conformation is adopted instantly (during 1–2 min) and no differences are detected in time for several hours (time dependence not shown in this work; unpublished results). At high bulk protein concentration (exceeding 10 mg/mL), ovalbumin retains its native structure at the interface. Similar behavior (retaining the secondary structure upon adsorption from higher bulk concentration) was observed previously with IRRAS for other proteins, like β -lactoglobulin (Meinders et al. 2001). This result has been explained by the fact that at high protein bulk concentration the degree of the surface coverage is already relatively high at the initial stage of the adsorption process. As a result, the adsorbing protein molecules are prevented from unfolding by the (already) apparent surface pressure of the molecules at the interface, leaving no opportunity for protein unfolding at interfaces, as has been discussed in the literature (Graham and Phillips 1979; Fainerman and Miller 1998). For example, lysozyme retains its catalytic activity (i.e. the enzyme native structure) adsorbed at surface pressures only higher than 8 mN/m (Graham and Phillips 1979; Fainerman and Miller 1998). Hence, the equilibrium surface protein concentration is not a nominator in the degree of unfolding at interfaces, but the initial concentration together with the kinetics of adsorption, as has been suggested previously (Pezennec et al. 2000).

Under equilibrium conditions, IRRAS data did not provide any indication for protein aggregation in the surface layer, based on the absence of anti-parallel β -structures in the protein (Fig. 4). Moreover, adsorption of pre-aggregated thermo-treated ovalbumin resulted in a partial deaggregation of the protein with kinetics on the hour timescale (E.V. Kudryashova, unpublished results), suggesting that the interface-adopted conformation is indeed a characteristic one.

Adsorption at the interface not only leads to partial unfolding but also to changes in protein mobility. The TRFA experiments show that ovalbumin rotates faster at the interface compared to the bulk solution (Table 2). Such behavior could be explained by a preferred molecular orientation at the interface. Ovalbumin has an ellipsoidal shape with an axial ratio of 1.3. The restriction in the ovalbumin mobility in “end-over-end” direction (i.e. about the short axis of the ellipsoid) could lead to a substantially shorter rotational correlation time. Such anisotropic motion of molecules with a non-spherical shape has been reported previously for a number of molecular systems (Harvey and Cheung 1977; Szabo 1984; Brand et al. 1985).

Compression of surface layers

To study the relationship between surface rheological properties and the protein structure, TRFA and IRRAS measurements were performed on-line upon compression of a protein surface layer that had been pre-equilibrated for 1 h. The pressure–area isotherm (Fig. 6) obtained is characterized by three stages: (1) initial compression coincides with a steady increase of the surface pressure; (2) a second stage after a ~ 1.5 -fold compression of the area where the surface pressure increases more sharply; up to (3) a point where collapse of the surface layer occurs. What are the changes in the molecular properties of the protein related to this surface pressure profile? Generally, compression of surface layers leads to a decrease in the molecular area available for a protein at the interface. This may induce the protein to (1) unfold, to (2) desorb from the interface or to (3) aggregate (Graham and Phillips 1979; Eastoe and Dalton 2000).

It was shown from IRRAS data that, during the first stage of compression (from 230 to 170 cm²), no significant further unfolding of the protein is observed with respect to the characteristic partially unfolded conformation of adsorbed ovalbumin in equilibrium (Fig. 7B). Changes in tertiary structure, however, cannot be excluded by the current technique. The surface protein concentration as well as the layer thickness change only slightly (Fig. 7A), and the “surface load” (i.e. layer thickness multiplied by surface concentration) remains constant. This implies that the protein has to desorb gradually from the interface into the bulk solution under the applied stress. During this stage of compression it was shown by IRRAS that the protein at the interface tends to aggregate (Fig. 8). The rotational correlation times are shown using TRFA measurements to become smaller (from 18 to ~ 8 ns). This corresponds, in our opinion, to the relatively fast rotation of protein segments, rather than the rotational motion of the whole molecule at the interface. The formation of protein aggregates, practically immobilized at the nanosecond time scale, but where segments still possess motional freedom, would explain such findings. Comparable

observations were made before for other proteins upon aggregation (Broos et al. 1995). The value of the rotational correlation time correlates with the degree of aggregation (estimated from IRRAS) and surface pressure in the initial stage of compression (Fig. 8), implying the relationship between these parameters. Altogether, the results suggest that compression-induced protein aggregation appears to be directly related to the surface pressure increase by means of altered protein–protein interactions.

While, in the initial stage of compression, material can still desorb from the surface, further reduction of the available area causes the partly aggregated proteins to establish enhanced interactions, prohibiting desorption. Also in this stage the “surface load” as defined above remains unchanged, since the increase in surface concentration is compensated by the decrease in layer thickness. The higher surface concentration, however, is a clear indicator for a more compact packing of the proteins at the interface, resulting in a still increasing anti-parallel β -sheet formation and increasing rotational correlation times. This, in turn, results in a sharp increase in the surface pressure and further collapse of the film (Fig. 6).

Conclusions

Detailed information on the molecular properties of the protein ovalbumin at the air/water interface was obtained in this work using a combination of external reflection IRRAS and TRFA methods, together with an on-line surface pressure measurement using a Langmuir balance. The TRFA method appears to be a promising technique to study the rotational dynamics of proteins at the air/water interface. It has also been found that ovalbumin adsorbed at the air/water interface adopts a characteristic partially unfolded conformation, yielding a 10% reduction of the β -sheet content. Despite the locally high protein concentration in the surface layer, the protein appears not to aggregate in equilibrium. The rotational dynamics of ovalbumin changed significantly at the interface. In contrast to the bulk solution, ovalbumin shows a more anisotropic motion, where the protein appears to have a restricted motion in end-over-end direction, which indicates a preferential orientation of the protein at the interface. Compression of surface layers of ovalbumin introduces aggregation of the proteins and the formation of a 2D network in the surface layer. The enhanced protein–protein interactions (resulting in anti-parallel β -sheet formation) correlates strongly with the increase in surface pressure upon compression, while the surface load (mg protein/m²) remains unchanged.

Thus, using a combination of two diverse advanced spectroscopic tools, molecular insight has been gained for proteins at the air/water interface under dynamic conditions. These results might help us to understand why foaming properties are protein specific. By studying a series of intrinsically modified proteins with altered

molecular functionality and by testing their behavior in equilibrium systems and monitoring their response to externally applied stress, we hope in the near future to contribute in clarifying the mechanism of foam formation and stabilization of relevance, for example, to the food industry.

Acknowledgements This research has been supported by a VLAG research school grant 2000 and by an INTAS grant YSF 2001/2-0147.

References

- Atkinson PJ, Dickinson E, Horne DS, Richardson RM (1995) Neutron reflectivity of adsorbed β -casein and β -lactoglobulin at the air/water interface. *J Chem Soc Faraday Trans* 91:2847–2854
- Bardwell JA, Dignam MJ (1985) Extensions of the Kramers–Kronig transformation that cover a wide range of practical spectroscopic applications. *J Chem Phys* 83:5468–5478
- Blaudez D, Boucher F, Buffeteau T, Desbat B, Grandbois M, Salesse C (1999) Anisotropic optical constants of bacteriorhodopsin in the mid-infrared: consequence on the determination of α -helix orientation. *Appl Spectrosc* 53:1299–1304
- Brand L, Knutson JR, Davenport L, Beechem JM, Dale RE, Walbridge DG, Kowalczyk AA (1985) Time-resolved fluorescence spectroscopy: some applications of associative behavior to studies of proteins and membranes. In: Bayley PM, Dale RE (eds) *Spectroscopy and the dynamics of molecular biological systems*. Academic Press, London, pp 259–305
- Bross J, Visser AJWG, Engbersen J, Verboom W, Van Hoek A, Reinhoudt D (1995) Flexibility of enzyme suspended in organic solvents probed by time resolved fluorescence anisotropy. Evidence that enzyme activity and enantioselectivity are directly related to enzyme flexibility. *J Am Chem Soc* 117:1637–1650
- de Jongh HHJ, Meinders MBJ (2002) Proteins at air/water interfaces studied using external reflection circular dichroism. *Spectrochim Acta A* 58:3197–3204
- Dickinson E, Horne DS, Phipps JS, Richardson RM (1993) A neutron reflectivity study of the adsorption of β -casein at fluid interfaces. *Langmuir* 9:242–248
- Digris AV, Skakun VV, Novikov EG, van Hoek A, Claiborne A, Visser AJWG (1999) Thermal stability of a flavoprotein assessed from associative analysis of polarized time-resolved fluorescence spectroscopy. *Eur Biophys J* 28:526–531
- Dong A, Meyer JD, Brown JL, Manning MC, Carpenter JF (2000) Comparative Fourier transform infrared and circular dichroism spectroscopic analysis of a1-proteinase inhibitor and ovalbumin in aqueous solution. *Arch Biochem Biophys* 383:148–155
- Eastoe J, Dalton JS (2000) Dynamic surface tension and adsorption mechanisms of surfactants at the air/water interface. *Adv Colloid Interface Sci* 85:103–144
- Elwing H (1998) Protein adsorption and ellipsometry in biomaterial research. *Biomaterials* 19:397–406
- Fainerman VB, Miller R (1998) Adsorption and interfacial tension isotherms for proteins. In: Möbius D, Miller R (eds) *Protein at liquid interfaces*. Elsevier, Amsterdam, pp 51–101
- Goormaghtigh E, Cabiliaux V, Ruyschaert J-M (1994) In: Hilderson HJ, Ralston GB (eds) *Subcellular biochemistry*, vol 23: physicochemical methods in the study of biomembranes. Plenum, New York, pp 405–450
- Graham DE, Phillips MC (1979) Proteins at liquid interfaces. II. Adsorption isotherms. *J Colloid Interface Sci* 70:415–426
- Graham DE, Phillips MC (1980) Proteins at liquid interfaces. II. Shear properties. *J Colloid Interface Sci* 76:240–250
- Gunning AP, Wilde PJ, Clark DC, Morris VJ, Parker ML (1996) Atomic force microscopy of interfacial protein films. *J Colloid Interface Sci* 183:600–602
- Harvey SC, Cheung HC (1977) Fluorescence depolarization studies on the flexibility of myosin rod. *Biochemistry* 16:5181–5187
- Harzallah B, Aguié-Beghin V, Douillard R, Bosi L (1998) A structural study of β -casein adsorbed layers at the air/water interface using X-ray and neutron reflectivity. *Int J Biol Macromol* 23:73–84
- Kopelman R, Tan W (1993) Near field optical microscopy, spectroscopy and chemical sensors. In: Morris MD (ed) *Microscopic and spectroscopic imaging of the chemical state*. Dekker, New York, pp 227–254
- Kudryashova EV, Gladilin AK, Izumrudov VA, van Hoek A, Visser AJWG, Levashov AV (2001) Formation of quasi-regular compact structure of poly(methacrylic acid) upon an interaction with chymotrypsin. *Biochim Biophys Acta* 1550:129–143
- Kudryashova EV, Gladilin AK, Levashov AV (2002) Proteins (enzymes) in supramolecular assemblies: investigation of structural organization by time-resolved fluorescence anisotropy. *Prog Biol Chem (Russ)* 42:257–294
- Lakowicz JR (1999) *Principles of fluorescence spectroscopy*, 2nd edn. Plenum, New York
- Meinders MBJ, de Jongh HHJ (2002) Limited conformational change of β -lactoglobulin upon adsorption at the air/water interface. *Biopolymers* 67:319–322
- Meinders MBJ, van den Bosch GGM, de Jongh HHJ (2000) IRRAS, a new tool in food science. *Trends Food Sci Technol* 11:218–225
- Meinders MBJ, van den Bosch GGM, de Jongh HHJ (2001) Molecular properties of proteins at and near the air/water interface from IRRAS spectra of protein solutions. *Eur Biophys J* 30:256–267
- Morrison LE, Weber G (1987) Biological membrane modeling with a liquid/liquid interface. Probing mobility and environment with total internal reflection excited fluorescence. *Biophys J* 52:367–379
- Novikov EG, van Hoek A, Visser AJWG, Hofstraat JW (1999) Linear algorithms for stretched exponential decay analysis. *Opt Commun* 166:189–198
- Pezenec S, Gauthier F, Alonso C, Graner F, Croguennec T, Brule G, Renault A (2000) The protein net electric charge determines the surface rheological properties of ovalbumin adsorbed at the air/water interface. *Food Hydrocolloids* 14:463–472
- Stein PE, Leslie AGW, Finch JT, Carell RW (1991) Crystal structure of uncleaved ovalbumin at 1.95 Å resolution. *J Mol Biol* 221:941–959
- Szabo A (1984) Theory of fluorescence depolarization in macromolecules and membranes. *J Chem Phys* 81:150–167
- Visser AJWG (1997) Time-resolved fluorescence on self-assembly membranes. *Curr Opin Colloids Interface Sci* 2:27–36
- Vos K, van Hoek A, Visser AJWG (1987) Application of a reference deconvolution method to tryptophan fluorescence in proteins. A refined description of rotational dynamics. *Eur J Biochem* 165:55–63
- Wustneck R, Kragel J, Miller R, Fainerman VB, Wilde PJ, Sarker DK, Clark DC (1996) Dynamic surface tension and adsorption properties of β -casein and β -lactoglobulin. *Food Hydrocolloids* 10:395–405
- Yamamoto K, Ishida H (1994) Optical theory applied to infrared spectroscopy. *Vibrational Spectrosc* 8:1–36